PKA regulates vacuolar H+-ATPase localization and activity via direct phosphorylation of the a subunit in kidney cells

Alzamora, R ; Thali, R F ; Gong, F ; Smolak, C ; Li, H ; Baty, C J ; Bertrand, C A ; Auchli, Y ; Brunisholz, R A ; Neumann, D ; Hallows, K R ; Pastor-Soler, N M

Abstract: The vacuolar H(+)-ATPase (V-ATPase) is a major contributor to luminal acidification in epithelia of Wolffian duct origin. In both kidney-intercalated cells and epididymal clear cells, cAMP induces V-ATPase apical membrane accumulation, which is linked to proton secretion. We have shown previously that the A subunit in the cytoplasmic V(1) sector of the V-ATPase is phosphorylated by protein kinase A (PKA). Here we have identified by mass spectrometry and mutagenesis that Ser-175 is the major PKA phosphorylation site in the A subunit. Overexpression in HEK-293T cells of either a wild-type (WT) or phosphomimic Ser-175 to Asp (S175D) A subunit mutant caused increased acidification of HCO(3)(-)-containing culture medium compared with cells expressing vector alone or a PKA phosphorylation-deficient Ser-175 to Ala (S175A) mutant. Moreover, localization of the S175A A subunit mutant expressed in HEK-293T cells was more diffusely cytosolic than that of WT or S175D A subunit. Acute V-ATPase-mediated, bafilomycin-sensitive H(+) secretion was up-regulated by a specific PKA activator in HEK-293T cells expressing WT A subunit in HCO(3)(-)-free buffer. In cells expressing the S175D mutant, V-ATPase activity at the membrane was constitutively up-regulated and unresponsive to PKA activators, whereas cells expressing the S175A mutant had decreased V-ATPase activity that was unresponsive to PKA activation. Finally, Ser-175 was necessary for PKA-stimulated apical accumulation of the V-ATPase in a polarized rabbit cell line of collecting duct A-type intercalated cell characteristics (Clone C). In summary, these results indicate a novel mechanism for the regulation of V-ATPase localization and activity in kidney cells via direct PKA-dependent phosphorylation of the A subunit at Ser-175.

DOI: https://doi.org/10.1074/jbc.M110.106278

JBC Papers in Press. Published on June 4, 2010 as Manuscript M110.106278
The latest version is at http://www.jbc.org/cgi/doi/10.1074/jbc.M110.106278

PKA REGULATES VACUOLAR H^+-ATPASE LOCALIZATION AND ACTIVITY VIA DIRECT PHOSPHORYLATION OF THE A SUBUNIT IN KIDNEY CELLS*

Rodrigo Alzamora[1], Ramon F. Thali[3], Fan Gong[1], Christy Smolak[1], Hui Li[1], Catherine J. Baty[2], Carol A. Bertrand[2], Yolanda Auchli[4], René A. Brunisholz[4], Dietbert Neumann[3], Kenneth R. Hallows[1,2#], and Núria M. Pastor-Soler[1,2]

From the [1]Renal-Electrolyte Division, Department of Medicine and [2]Department of Cell Biology and Physiology, University of Pittsburgh School of Medicine, Pittsburgh, PA 15261; [3]Department of Biology, Institute of Cell Biology, ETH Zurich, 8093 Zurich; and [4]Functional Genomics Center Zurich (FGCZ), University of Zurich, 8057 Switzerland.

Running head: PKA phosphorylation and regulation of V-ATPase in kidney

[#]Address correspondence to: Kenneth R. Hallows, M.D., Ph.D., Renal-Electrolyte Division, Department of Medicine, S976.1 Scaife Hall, 3550 Terrace Street, Pittsburgh, PA 15263. Tel: 412-648-9580. Fax 412-383-8956; E-mail: hallows@pitt.edu

The vacuolar H^+-ATPase (V-ATPase) is a major contributor to luminal acidification in epithelia of Wolffian duct origin. In both kidney intercalated cells and epididymal clear cells, cAMP induces V-ATPase apical membrane accumulation, which is linked to proton secretion. We have shown previously that the A subunit in the cytoplasmic V_1 sector of the V-ATPase is phosphorylated by PKA. Here we have identified by mass spectrometry and mutagenesis that Ser-175 is the major PKA phosphorylation site in the A subunit. Overexpression in HEK-293T cells of either a wild-type (WT) or phospho-mimic Ser-175 to Asp (S175D) A subunit mutant caused increased acidification of HCO_3^--containing culture media compared to cells expressing vector alone or a PKA phosphorylation-deficient Ser-175 to Ala (S175A) mutant. Moreover, localization of the S175A A subunit mutant expressed in HEK-293T cells was more diffusely cytosolic than that of WT or S175D A subunit. Acute V-ATPase-mediated, bafilomycin-sensitive H^+ secretion was up-regulated by a specific PKA activator in HEK-293T cells expressing WT A subunit in HCO_3^--free buffer. In cells expressing the S175D mutant, V-ATPase activity at the membrane was constitutively up-regulated and unresponsive to PKA activators, while cells expressing the S175A mutant had decreased V-ATPase activity that was unresponsive to PKA activation. Finally, Ser-175 was necessary for PKA-stimulated apical accumulation of the V-ATPase in a polarized rabbit cell line of collecting duct A-type intercalated cell characteristics (Clone C). In summary, these results indicate a novel mechanism for the regulation of V-ATPase localization and activity in kidney cells via direct PKA-dependent phosphorylation of the A subunit at Ser-175.

V-ATPases are ubiquitous and essential transport protein complexes that acidify many cellular organelles, such as endosomes, lysosomes and the Golgi complex (1). The V-ATPase has 14 subunits distributed into two domains. The V_1 peripheral or cytoplasmic domain, which catalyzes ATP hydrolysis, is composed of eight different subunits, including subunit A (reviewed in (2)). The V_0 integral membrane domain, which is responsible for H^+ translocation, consists of six different subunits, including subunit *a* (2). Some epithelial cells, such as kidney proximal tubular cells, A-type intercalated cells, and epididymal clear cells express abundant V-ATPase at their apical membrane, where it participates in endocytosis and luminal acidification of the kidney tubule and the male reproductive tract, two epithelia of Wolffian duct origin (3-7). V-ATPase dysfunction in kidney cells has been implicated in the development of Fanconi syndrome and renal tubular acidosis, with severe kidney and generalized health sequelae (8-13). In mice, a lack of V-ATPase expressing clear cells leads to male infertility (14).

Acid secretion in epithelial cells is actively regulated by environmental signals, although the mechanisms by which these cues are translated into activation of H^+ transport pathways remains the subject of intense research (11,15-19) For example, the V-ATPase is regulated by several pathways, which involve CO_2,

phosphatidylinositol 3-kinase, aldolase, phosphofructokinase, actin, microtubules, and angiotensin in a variety of mammalian cellular systems (20-27). The number of V-ATPases at the apical membrane of intercalated cells in the kidney increases rapidly under conditions of systemic acidosis (28,29). Acidosis also induces H^+ secretion via the V-ATPase through changes in intracellular [Ca^{2+}] concentration, calmodulin activation, the cytoskeleton, and by altering the rate of endocytosis and exocytosis in kidney cells (30).

We and others have shown that regulation of the V-ATPase at the apical membrane of intercalated and clear cells is tightly linked to alkaline luminal pH, HCO_3^-, carbonic anhydrase activity, activation of the soluble Adenylyl Cyclase (sAC), cAMP, and PKA (19,31-33). In cells with abundant carbonic anhydrase, such as intercalated cells, increases in extracellular CO_2 during acidosis may result in significant transient increases in intracellular [HCO_3^-] and [H^+]. Increased [HCO_3^-] may in turn activate the sAC/cAMP/PKA pathway and the V-ATPase at the apical membrane of A-intercalated cells resulting in enhanced proton extrusion and subsequent basolateral recovery of HCO_3^- into the extracellular space (19).

The role of direct phosphorylation of the V-ATPase subunits in H^+ secretion in mammalian epithelial cells has not been well characterized (19,34,35). Although PKA agonists have been shown to regulate the V-ATPase in a variety of systems, it was not until recently that the direct phosphorylation of V-ATPase subunits by this kinase was linked to its regulation. In insect cells phosphorylation of the C subunit in the V_1 sector by PKA contributes to the apical assembly and activity of the salivary gland V-ATPase (36,37). We have recently shown that the V-ATPase A subunit is phosphorylated by PKA in vitro and in the intact cellular environment in HEK-293 cells, suggesting that direct A subunit phosphorylation by PKA could be involved in the trafficking of the V-ATPase complex to the apical membrane from cytoplasmic pools (19,38,39).

In this study we have used mass spectrometry and phosphorylation assays to identify and confirm the main PKA phosphorylation site in the V-ATPase A subunit, which is highly conserved across species. Moreover, we have established the relevance of this residue in the phosphorylation of the A subunit in HEK-293 cells that express native and active V-ATPase at their plasma membrane (40). We have also developed a useful technique to monitor V-ATPase activity in live cells and to test for the effects of mutations in the pump A subunit. Moreover, we have used established morphometric methods to confirm that this PKA phosphorylation site is required for apical accumulation of the pump in response to PKA activators in the Clone C cell line, a previously characterized rabbit cell line of kidney intercalated cell characteristics that expresses V-ATPase.

EXPERIMENTAL PROCEDURES

Reagents and chemicals. All chemicals used in the studies presented here were purchased from Sigma or Fisher Scientific unless otherwise stated. The cell-permeant PKA-specific activator N^6-monobutyryl-cAMP (6-MB-cAMP) was obtained from Biomol.

Mass spectrometry of wild-type mouse FLAG-A V-ATPase subunit. The wild-type (WT) mouse FLAG-A subunit construct characterized in our previous study (19) was transfected into HEK-293T cells and immunoprecipitated using the M2 anti-FLAG monoclonal antibody (Sigma) coupled to protein A/G beads (Pierce), as described (19,41,42). This FLAG-WT-A V-ATPase subunit was phosphorylated by bacterially expressed active PKA (43) at 37°C in kinase buffer (10 mM HEPES-Cl, pH 7.4, 200 µM ATP, 40 µM AMP, 5 mM $MgCl_2$) supplemented with [γ-^{32}P]-ATP for 2 h. The reaction was stopped by adding SDS-containing sample buffer and heating to 95°C for 5 min. The following steps were performed as described previously (43) with only one minor modification. Briefly, following SDS–polyacrylamide gel electrophoresis (PAGE) and Coomassie-blue staining, the gel band corresponding to the FLAG-A V-ATPase subunit was excised from the wet gel and subjected to in-gel digestion with trypsin. Concentrated tryptic peptides were applied to a microbore reversed-phase column connected to a capillary liquid chromatography system and equipped with a microcollection/spotting system, thus allowing the microfractionation onto a Prespotted AnchorChip (PAC) (44). After autoradiography, selected fractions of the PAC target indicating the presence

of radiolabeled phosphopeptides were analyzed by matrix-assisted laser desorption ionization mass spectrometry (MALDI MS) (44).

To confirm the phosphorylation site identified by mass spectrometry analysis, the candidate phosphorylation site was mutated using the Stratagene QuikChange kit according to the manufacturer's instructions using as a template the pMO-FLAG-A plasmid, which we have used for mammalian cell expression (38). All mutations were confirmed by DNA sequencing.

A subunit in vitro phosphorylation assays. In vitro phosphorylation assays were performed essentially as described previously (38,41). Briefly, HEK-293T cells were transiently transfected using Lipofectamine 2000 (Invitrogen) to express either FLAG-V-ATPase A subunit wild-type (FLAG-A-WT, mouse sequence) or this subunit with a specific point mutant (Ser-175 to Ala; FLAG-A-S175A) identified as the PKA target phosphorylation site. Cells were lysed two days after transfection, and the FLAG-V-ATPase A subunits (WT and S175A) were immunoprecipitated from cell lysates using the M2 anti-FLAG monoclonal antibody (Sigma) coupled to protein A/G beads (Pierce). In vitro phosphorylation was performed using purified active PKA catalytic subunit (Promega) with [γ-^{32}P]-ATP labeling, as described (38). After SDS-PAGE and transfer to nitrocellulose membranes, immunoblotting for expression of FLAG-V-ATPase A subunit was first performed and quantified using a Versa-Doc Imager with Quantity One software (Bio-Rad). After the chemiluminescent signal decayed, phosphorylated bands on the membrane were identified by exposure of the same membrane to a phospho-screen, and the detected bands were quantitated using a Bio-Rad Phosphorimager with Quantity One software. The intensity of each phospho-screen band was corrected by subtracting out the local background in the same lane.

A subunit in vivo phosphorylation assays. HEK-293T cells were transiently transfected with 3 μg of either WT or S175A mutant FLAG-V-ATPase A subunit plasmid DNA one day before experimentation. Phosphorylation assays in HEK-293T cells were performed essentially as previously described (38). In addition, to assess potential differences in PKA-mediated [^{32}P]-orthophosphate labeling in the cells across conditions, 10 μg of lysate was pre-cleared by incubation with protein A/G beads (approximately 1.5 μL) and then spotted for each condition onto a nitrocellulose membrane. The [^{32}P]-orthophosphate-labeled proteins in each spot were detected by exposing the membranes to a phospho-screen and quantified using a phosphorimager. Thereafter, the membranes were blocked in 5% BSA in TBST and probed with an antibody recognizing a phosphorylated PKA consensus epitope (1:15,000; Cell Signaling Technologies) to account for potential differences in PKA activity modulation across conditions. Finally, membranes were stripped and re-probed using an anti-β-actin antibody (Sigma) to normalize for any differences in total protein content in the spotted samples. The total [^{32}P]-orthophosphate and PKA phosphorylated substrate signals were corrected for the local background signal and normalized to the β-actin immunoblot signal in each spot. Each experimental condition was repeated three times for each V-ATPase A subunit construct. Measurements were analyzed and graphed as mean ± SEM.

Immunofluorescence labeling of HEK-293T cells transfected with V-ATPase A subunit mutants. HEK-293T cells were seeded onto poly-L-lysine coated coverslips at 2.5 x 10^5 cells/cm^2, and transfected with either pMO vector alone or pMO-FLAG-A-WT, -FLAG-A-S175A (Ser-175 to Ala), or -FLAG-A-S175D (Ser-175 to Asp) A subunit using the techniques described above for phosphorylation experiments. At least three independent coverslips were used in immunolabeling experiments for each group of transfections (either vector alone, WT, S175A, or S175D A subunit). Cells on coverslips were incubated for 5 min in concanavalin A coupled to CY3 (Vector Laboratories) diluted at 1: 200 for 5 min in PBS pH 7.4 at 37ºC followed by a brief wash in PBS as described (45). All antibodies were diluted in DAKO diluent (DAKO Laboratories) at various concentrations. The coverslips were fixed in 2% paraformaldehyde in PBS for 30 min and immunolabeled using an anti-FLAG antibody raised in mouse (M2 anti-FLAG) for 60 min at room temperature (1:50 dilution), followed by incubation in secondary goat anti-mouse antibody coupled to Alexa 488 (1:800 dilution; Jackson Immunologicals) for 60 min, and

then TO-PRO-3 (Invitrogen, 1:400 in PBS) to stain the nuclei for 5 min, using our previously published protocol in other cell lines (46). Images from these coverslips were acquired with identical laser confocal microscope settings across all transfection conditions. Images were imported into Adobe Photoshop for presentation as described previously (38).

Measurement of changes in extracellular media pH (pH_o). HEK-293T cells were passaged every 24-36 h for one week and then seeded onto poly-L-lysine-coated 24-well plates at an initial concentration of 2.5 x 10^5 cells/well. The cells were transiently transfected the next day with 0.3 µg/well of plasmid DNA (either vector alone, WT, S175A, or S175D; 6 wells per DNA sample). Transfected cells were grown in high-glucose, bicarbonate-containing DMEM media (Invitrogen) supplemented with 10% FBS at 37°C in the presence of 5% CO_2/95% air. At 28-31 h after transfection the medium from each well was collected, and its pH was measured using a pH meter (Fisher) after careful equilibration of the sample with 5% CO_2/95% air. Cells were then incubated for 5 min at 37°C in 1 mL of a Na^+-free, low buffering capacity solution containing (in mM): 135 N-methyl-D-glucamine, 5 KCl, 2 $CaCl_2$, 1.2 $MgSO_4$, 5.5 D-glucose, 6 L-Alanine, 4 lactic acid, 1 HEPES, titrated to pH 7.43 using 1 HCl (modified from (47)). The solutions from each well were replaced with 1 mL of fresh solution and then incubated for 7 min at 37ºC before collecting them for pH_o measurements, which were also performed at 37ºC. This procedure (7-min incubation followed by pH_o measurement) was repeated two more times for each well either in the presence of vehicle or of 100 µM 6MB-cAMP / 500 µM IBMX. Reported acidification rates (in pH units/min) were calculated from the pH drop of the solutions (final minus initial pH) over the third 7-min incubation period. After these incubations the same procedure was repeated with three successive 7-min incubations in the presence of 1 µM bafilomycin A1. The V-ATPase-dependent rate of pH_o acidification for each sample well was defined as the difference in the acidification rate measured in the absence versus the presence of bafilomycin A1 (i.e., bafilomycin A1-sensitive pH acidification rate). Comparing extracellular pH change rates originating from the same starting pH in the absence vs. presence of bafilomycin allowed us to quantify the V-ATPase-dependent extracellular acidification rate within the same tissue culture well within a short period of time. The time frame for action of bafilomycin in these cells was ~12-30 min, as evidenced by a significant inhibition of extracellular acidification starting at ~12 min, and an increase in cell death after ~30 min. Thus, by comparing the third of three 7-min incubations both in the absence and presence bafilomycin, we obtained the extracellular acidification rates in the window of time where bafilomycin is active against the V-ATPase but not yet significantly toxic to the cells.

At the end of each experiment cells were collected to determine total cell number, as counted with a hemocytometer, and cell viability, as assessed by Trypan blue exclusion. We prepared at least 12 wells of cells for each plasmid type expressed (vector alone, WT, S175A and S175D), and half of those wells were treated with PKA agonist and the other half with buffer alone. To assess FLAG-A subunit expression in the transfected cells, we immunoblotted cell lysates at the end of the pH_o experiments using both anti-FLAG and anti-β-actin antibodies, as described above. In addition, we performed dot blots of these cell lysates using the anti-PKA substrate antibody to confirm PKA activity changes in these cells with the different treatments, as described above.

Immunofluorescence labeling of V-ATPase FLAG-A subunit mutants transiently transfected into a cell line of intercalated cell characteristics. We used a previously characterized rabbit cell line ("Clone C", a generous gift of Dr. Qais Al-Awqati), which displays kidney collecting duct intercalated cell characteristics (48,49). This cell line expresses high levels of functional V-ATPase at the apical membrane when cells are seeded at high density. Briefly, Clone C cells were grown at 32ºC in medium containing DMEM/F12 (Invitrogen), 1.8% heat-inactivated fetal calf serum, 27.6 µM hydrocortisone (Sigma), 0.45% insulin-transferrin-sodium selenite media supplement (Sigma), 15 mg/L epidermal growth factor (Sigma), 200 mM glutamine (Sigma), and 5% penicillin/streptomycin (Invitrogen) as previously described (50). Cells were placed into serum and antibiotic-free medium for 4 h prior to transfection. The cells were then transiently transfected according to the manufacturer's recommendations using Lipofectamine 2000 with

either FLAG-A-WT or FLAG-A-S175A (3 μg plasmid DNA). One day after transfection, cells were plated under conditions that confer apical V-ATPase proton secretion (51) onto 0.33-cm^2 Transwell filters (Costar) coated with rat tail collagen (BD Biosciences) at a concentration of 5 x 10^5 cells per cm^2 and grown at 40ºC in DMEM medium with 1.8% FBS (52).

Five days after transfection, monolayers on filters were incubated in serum-free DMEM for 2 h and then treated with either vehicle or 1 mM 6-MB-cAMP and 0.5 mM IBMX for 30 min at 40ºC in PBS at pH 7.1. After treatment with agonists, cells on filters were incubated in CY3-concanavalin A (1:100) in PBS at 40ºC. After a brief PBS wash, cells were fixed and immunolabeled using the M2 anti-FLAG antibody, followed by a secondary antibody coupled to Alexa-488 (GAM-Alexa 488; 1:50, Invitrogen) and the nuclear label TO-PRO-3 using the same protocol as described above for HEK-293T cells. Filters were imaged from above the first appearance of apical fluorescence down to below the lowest basolateral fluorescence labeling using a Leica confocal microscope. For each set of filters the stacks were acquired using identical stack dimensions and Z-steps using a 40X objective (zoom 3). Transfected cells on the filters were selected when they showed both concanavalin A and bright anti-FLAG immunolabeling by epifluorescence. Approximately 30% of the cells in the monolayers fulfilled these characteristics. At the time of selection of the transfected cells (as determined by their bright FITC-associated fluorescence) for imaging and acquisition of the stacks, investigators were unable to judge the subcellular localization of the V-ATPase. Three-dimensional reconstructions of confocal stacks were used to obtain X-Z or X-Y projections of the transfected cells in the monolayers, which were then imported into Metamorph for quantification. V-ATPase apical accumulation was determined by measuring the mean pixel intensity (MPI) of FLAG-associated fluorescence in an apical ROI (ROI-1, co-localizing with CY3-concanavalin A) and a cytoplasmic ROI of identical size immediately below concanavalin A labeling (ROI-2), using a very similar procedure to ones previously described by us (19,38,53). The brightest area of the cell at the apical membrane was chosen for measuring the ROI-1 (approximately, 200 pixels). After X-Z reconstruction, at least two additional investigators blinded as to the nature of the transfected subunits evaluated the distribution of anti-FLAG labeling in TIF images of these cells. The degree of apical accumulation of the V-ATPase FLAG A subunit mutants was determined by the ratio of apical-to-cytoplasmic ROI (ROI-1/ROI-2) of FLAG-associated fluorescence for each cell. At least five separate Clone C filters were evaluated for each of four conditions: FLAG-A-WT incubated in PBS pH 7.1 ± 6-MB-cAMP / IBMX and FLAG-A-S175A incubated in PBS pH 7.1 ± 6-MB-cAMP / IBMX. For each of these four studied conditions in Clone C monolayers, we quantified 20-45 cells.

Co-immunoprecipitation studies. Clone C cells were transfected with FLAG-WT A subunit plasmid as described above. One day after transfection, cells were harvested in ice-cold lysis buffer using our established techniques (41). We used 1 mg of pre-cleared lysate for immunoprecipitations performed at 4°C on each sample using the M2 anti-FLAG antibody (0.5 μg/immunoprecipitation) coupled to protein A/G beads. As a control, immunoprecipitation in the absence of the anti-FLAG antibody was also performed. After three washes in lysis buffer, the immunoprecipitation samples were eluted in sample buffer and, along with the cell lysate samples, subjected to SDS-PAGE. Immunoblotting was performed with either: 1) V_0 *a* subunit antibody (1:2,000 dilution, raised in rabbit, Santa Cruz), 2) V_1 A subunit antibody (1:5,000 dilution, raised in chicken, Sigma) or 3) V_1 E subunit antibody (1:10,000 dilution, raised in chicken, Sigma), followed by the appropriate secondary antibodies coupled to HRP (Jackson Immunologicals) (38).

Statistics. Data shown represent means ± SEM for each group. Significance was determined using two-tailed, unpaired Student's t-tests assuming unequal variances between the treatment groups. *P* values <0.05 were considered significant.

RESULTS

PKA phosphorylates the V-ATPase A subunit at Ser-175. We have previously shown that the V-ATPase A subunit can be phosphorylated both in vitro and in vivo by AMPK and PKA when

heterologously expressed in HEK-293 kidney cells (38). However, actual PKA phosphorylation sites within the A subunit have not yet been identified. Using a novel approach involving a liquid chromatography matrix-assisted laser desorption/ionization mass spectrometry (LC–MALDI MS) workflow, we were able to localize and quantify phosphorylated peptides on a MALDI target plate prior to MS analysis (43). Using this technique with in vitro PKA-phosphorylated V-ATPase FLAG-tagged A-WT subunit, we identified a major phospho-labeled tryptic peptide fragment that eluted in fraction O21 (Figs. 1A and 1B). In this elution peak we detected a phosphorylated peptide corresponding to the expected molecular mass of a tryptic fragment with sequence NRG**S**VTYIAPPGNYDASDVVLELEFEGVK, for which sequence confirmation was obtained by fragmentation using MS/MS (see Supplemental Data, Fig. S1). This peptide fragment (underlined in Fig. 1C) contains two serines, however only Ser-175 (bolded in Fig. 1C) fits within a consensus PKA phosphorylation site. The amino acid sequence around this residue is highly conserved in vertebrates (Fig. 1D), suggesting that PKA phosphorylation at this site could play a fundamental role in V-ATPase function.

To further confirm that Ser-175 is a specific PKA phosphorylation site in vitro, we generated a putative phosphorylation-deficient FLAG-tagged A-subunit mutant with Ser-175 mutated to Ala (S175A) and then performed in vitro phosphorylation experiments, using methods previously described (38). We then compared in vitro phosphate labeling of WT vs. the S175A V-ATPase A subunits exposed to purified active PKA catalytic subunit in the presence of [γ-^{32}P]-ATP (Figs. 2A and 2B). The S175A V-ATPase A subunit mutant had a >90% reduction in ^{32}P labeling relative to WT A subunit after normalization to the amount of immunoprecipitated protein, confirming PKA-dependent phosphorylation at this residue in vitro. Together, the mass spectrometry analysis and in vitro phosphorylation results reveal that PKA phosphorylates the V-ATPase subunit at this highly conserved site in mammalian and other vertebrate animals.

PKA-dependent in vivo phosphorylation of the V-ATPase A subunit in HEK-293T cells occurs at Ser-175. To determine whether Ser-175 is a target for PKA-dependent phosphorylation in intact HEK-293T cells, we compared [^{32}P]-orthophosphate labeling of the FLAG-A-WT and FLAG-A-S175A mutant subunits under control conditions or following treatment with PKA activators (100 µM 6-MB-cAMP + 500 µM IBMX) or a specific PKA inhibitor (10 µM mPKI) (Fig. 3A). The phosphate-labeling signal on the phospho-screen (upper panel) was normalized to the respective FLAG-A subunit expression signal on the immunoblot (lower panel) from the same membrane.

Stimulation of cellular PKA activity by PKA activators significantly increased phosphorylation of the FLAG-A-WT subunit to ~3.5 times that of control-treated cells (Fig. 3B, lanes 1 and 2). Treatment with the PKA inhibitor mPKI did not significantly decrease the level of WT A-subunit phosphorylation compared with untreated cells, although there was an inhibitory trend with mPKI treatment (Fig. 3B, lanes 1 and 3). The changes in WT and mutant A subunit phosphorylation with PKA modulation were qualitatively similar to the changes in overall cellular PKA-phosphorylated substrates, as measured by a dot blot detecting PKA-phosphorylated proteins in the total cellular lysate (compare Fig. 3B, lanes 1-3, with Fig. 3D, lanes 1-3). These results are consistent with our earlier published results on WT A subunit phosphorylation by PKA in cells (38).

Untreated cells expressing the S175A A subunit mutant had ~50% lower phosphorylation levels compared with untreated cells expressing the WT A subunit (Figs. 3A and 3B, lanes 1 and 4). This result indicates that Ser-175 in the A subunit is likely a target of baseline phosphorylation in unstimulated cells. Moreover, the robust enhancement in phosphorylation of the FLAG-A-WT subunit following PKA stimulation was completely blocked in the FLAG-A-S175A mutant subunit (compare Figs. 3A and 3B, lanes 1 and 2 with lanes 4 and 5). This blockade could not be attributed to a lack of PKA activation in the S175A mutant subunit-expressing cells, as total cellular PKA-phosphorylated substrates approximately doubled with PKA stimulation in both WT- and mutant A subunit-expressing cells (Fig. 3D, lanes 2 and 5). Together, these results strongly indicate that Ser-175 in the V-ATPase A subunit is the main target of PKA phosphorylation

in vivo (i.e., in an intact cellular environment).

Ser-175 is required for V-ATPase subcellular localization and activity in HEK-293T cells. HEK-293 cells express the V-ATPase at their plasma membrane, where it has been shown to extrude protons (40). Lang et al. demonstrated that other H^+-secreting transporters, such as Na^+/H^+ exchangers (NHEs), are not active in HEK-293 cells with neutral to alkaline intracellular pH (40). To examine the subcellular localization of the V-ATPase A subunit expressed in HEK-293T cells, a commercially-available subclone of HEK-293 cells (45), we transfected these cells with either FLAG-tagged WT or mutant A subunits. We then performed immunofluorescence labeling of the A subunit immediately after removing the cells from culture medium using an anti-FLAG antibody followed by confocal fluorescence microscopy (Fig. 4, A-D). Cells transfected with either FLAG-A-WT or with FLAG-A-S175D exhibited immunolabeling largely at or near the plasma membrane (co-labeled with concanavalin A-CY3, in red), with less prominent cytosolic staining (Fig. 4, B and D). However, HEK-293T cells transfected with FLAG-A-S175A displayed a more predominant cytosolic distribution than HEK-293T cells expressing WT or S175D A subunits (Fig. 4C). Immunolabeled cells that were transfected with vector alone showed very little non-specific staining (Fig. 4A). All confocal images shown were acquired using identical laser settings in cells that immunolabeled on the same day under the same conditions. Together, these results suggest that phosphorylation at Ser-175 in the A subunit may play a functional role in the subcellular distribution of the V-ATPase in these cells.

To more directly assess the role of A subunit residue Ser-175 in the activity of the V-ATPase at the plasma membrane, we transfected HEK-293T cells with either vector alone, WT, or mutant A subunits (S175A or S175D), incubated in the same volume of culture medium and then measured the extracellular pH (pH_o) of the medium 28-31 h after transfection (Fig. 4E). Fresh HEK-293T cell culture medium had a measured pH of 7.48 ± 0.01 at 37°C in a 5% CO_2 environment. In cells transfected with either vector alone or the PKA phosphorylation-deficient S175A A-subunit mutant, only modest acidification of the media occurred over the subsequent 28-31 h (to a pH_o of 7.33-7.35; Fig. 4E, lanes 1 and 3). Expression of the WT A subunit significantly enhanced acidification of the medium relative to vector alone (to a pH_o of 7.17 ± 0.02; Fig. 4E, lane 2). Finally, expression of the phospho-mimic S175D A-subunit mutant caused an even more profound and significant acidification of the culture medium (to a pH_o of 7.03 ± 0.02; Fig. 4E, lane 4). Thus, the degree of media acidification observed after transfection of WT and Ser-175 mutant A subunits into HEK-293 cells (Fig. 4E) were consistent with qualitative changes in expression of the transfected subunits at or near the plasma membrane (Figs. 4A-4D). The total cell number, as counted on a hemocytometer at the end of each experiment, and viability, as measured by Trypan blue exclusion, did not differ significantly across transfection conditions (between 0.99 x 10^6 and 1.10 x 10^6 cells per well and between 94.1 and 95.6% cell viability across all transfection conditions). Moreover, nuclear staining did not reveal blebbing of cell nuclei under any of the conditions tested (Figs. 4A-4D), which suggests that apoptosis was not occurring to a significant extent (54). Expression levels of FLAG-tagged A subunits in transfected cells were quite comparable, as demonstrated in the immunoblots of the phosphorylation experiments in intact HEK-293T cells (Fig. 3). These considerations suggest that changes in media pH in cultures were not due to differences in cell death, growth rates, transfected subunit expression levels, or plating across conditions.

In additional experiments we monitored pH_o changes under acute conditions (over 7-min intervals) in HEK-293T cells seeded at equal densities into 24-well plates and transfected with either vector alone or plasmid to express WT, S175A or S175D mutant A subunit (Fig. 5). V-ATPase-dependent acidification was measured as described in *Experimental Procedures* after replacing the culture medium with a low buffering capacity solution. This buffer was prepared without Na^+ to minimize any contribution of Na^+/H^+ exchange to pH_o and in the nominal absence of HCO_3^- to minimize sAC activity, which could independently increase intracellular [cAMP] and PKA activity (31,40,55). We confirmed that HEK-293T cells incubated in this weakly buffered solution express sufficient V-ATPase at their plasma membrane to generate significant changes

in pH_o. When comparing untreated (Fig. 5A) vs. 6-MB-cAMP-treated cells (Fig. 5B), only over-expression of the WT A subunit caused a significant change in the V-ATPase-dependent acidification rate (expressed as [-(final buffer pH - initial buffer pH)/Δt]). Specifically, expression of vector alone and S175A maintained relatively low acidification rates, and S175D maintained a high acidification rate under both untreated and PKA-stimulated conditions. On the other hand, the WT A subunit had a low acidification rate under untreated conditions that converted to a high acidification rate in the presence of the PKA activators 6-MB-cAMP and IBMX. Comparing the different transfection conditions in cells incubated with buffer alone (untreated), only vector alone and S175A had V-ATPase-dependent acidification rates that were not statistically different from one another. The relative measured acidification rates were: vector $\simeq$ S175A < WT < S175D (Fig. 5A). Comparing the different transfection conditions in the presence of the PKA activators, both vector alone vs. S175A and WT vs. S175D had V-ATPase-dependent acidification rates that were not statistically different from one another. The relative measured acidification rates with PKA stimulation were: vector $\simeq$ S175A < WT $\simeq$ S175D (Fig. 5B). Of note, as observed in Fig. 3, during the time frame of these pH_o measurements, there was comparable expression of each FLAG-A subunit, and the level of total PKA-phosphorylated substrate in cells significantly increased with 6-MB-cAMP and IBMX treatment (data not shown). Taken together, the results presented so far suggest that PKA-mediated phosphorylation of the A subunit at Ser-175 in HEK-293T cells may be both necessary and sufficient to confer V-ATPase activity at the plasma membrane under conditions that minimize intracellular HCO_3^- and the contribution to H^+ secretion by NHEs. In the presence of bafilomycin and in the absence of Na^+, we still observed a slight but consistent drop in pH_o (Fig. S2) which could be due to other Na^+-independent, H^+-extruding transporters, such as the H^+-monocarboxylate co-transporters of the SLC16 family, which are known to be expressed in the HEK-293 cell line (56,57).

Ser-175 is required for PKA-mediated V-ATPase A-subunit apical accumulation in Clone C intercalated cells. To evaluate the role of PKA-dependent phosphorylation at Ser-175 in the A subunit vis-à-vis subcellular localization changes of the V-ATPase in a more physiologically relevant cell system, we expressed the FLAG-A subunit in a rabbit cell line of intercalated cell characteristics, Clone C. This cell line has been previously characterized and, when plated at high density, expresses active V-ATPase at the apical membrane (49). First, we performed co-immunoprecipitation experiments to determine whether the exogenously expressed FLAG-A-WT subunit incorporates into endogenous V-ATPase complexes. As demonstrated by immunoblotting with specific antibodies that recognize endogenous V-ATPase subunits, we confirmed that both the V-ATPase *a* subunit of the membrane-embedded V_o sector (Fig. 6A, upper panels) and the E subunit of the V_1 sector (Fig. 6A, lower panels) co-immunoprecipitated with transfected FLAG-A-WT subunit expressed in Clone C cells (Fig. 6A, middle panel).

Next, we performed immunofluorescence labeling of V-ATPase FLAG-A-WT or S175A mutant subunit expressed in polarized Clone C cells followed by confocal microscopy. The FLAG-A-WT subunit was distributed in both apical and cytosolic domains when expressed in Clone C cells and incubated in PBS at pH 7.1 (Fig. 6B, left upper panel). Under this incubation condition we minimized any exposure of the cells to hormones and agonists present in serum (by serum starving the monolayers for 2 h), which could potentially influence intracellular cAMP/PKA. The use of PBS pH 7.1 during the incubation also minimized HCO_3^--induced trafficking of the V-ATPase in proton-secreting cells as previously described (31). When Clone C cells expressing the FLAG-A-WT subunit were treated with the PKA activators 6-MB-cAMP and IBMX, these cells accumulated FLAG-associated fluorescence at their apical poles (Fig. 6B, upper right panel). In contrast, the FLAG-A-S175A mutant subunit showed a more diffuse cytoplasmic distribution both in the presence and absence of PKA agonists (Fig. 6B, lower panels).

Quantification of the apical-to-cytoplasmic MPI of FLAG-associated fluorescence in Clone C cells transfected with WT vs. S175A A subunit confirmed a significantly lower apical accumulation of the S175A A-subunit mutant (Fig. 6C), and its unresponsiveness to trafficking to the apical membrane by PKA agonists. Our

quantification also reveals that transfected FLAG-A-WT subunit in Clone C cells traffics to the apical membrane in the same 30-min time frame that the E subunit accumulates at the apical membrane of intercalated cells in kidney tissue slices in response to 6-MB-cAMP (19,39). In summary, these results suggest that phosphorylation at Ser-175 is required for the PKA-mediated apical accumulation in polarized kidney intercalated cells.

DISCUSSION

An area of particular research interest in kidney and epithelial cell physiology is in the understanding of how changes in intracellular and extracellular pH are sensed acutely by proton-secreting cells and translated into the activation of transporters such as the V-ATPase (17,32). It has been shown that V-ATPase subcellular localization and/or V-ATPase-dependent proton secretion are regulated by a variety of stimuli, including changes in intracellular and extracellular pH, extracellular [CO_2], intracellular [Ca^{2+}], and [HCO_3^-] in proton-secreting cells derived embryologically from the Wolffian duct (20,51,58,59). Carbonic anhydrase and sAC are very abundant in kidney intercalated cells, where sAC activation generates cAMP upon increases of CO_2 that may occur under conditions of acute respiratory acidosis (31,60). We envision that in response to an acute intracellular increase of [CO_2], HCO_3^- production catalyzed by carbonic anhydrase in the intercalated cell (11,58) would generate cAMP via sAC and thereby induce acute PKA-dependent trafficking of the V-ATPase to the apical membrane for rapid proton secretion (19).

To date, the mechanisms of kinase-dependent regulation of V-ATPase trafficking in mammalian cells have been unknown (34,38,61). Our previous work demonstrated that direct phosphorylation of the V-ATPase A subunit occurred in HEK-293 cells, and we proposed that such phosphorylation could potentially play an important role in the regulation of subcellular localization and activity of the V-ATPase in kidney intercalated cells (19,38,39). This mode of regulation of V-ATPase activity could also prove to be relevant in the proximal tubule of the kidney to the extent that PKA or other relevant kinases may become activated there. However, the levels of sAC in the epithelium of that nephron segment are lower than in the collecting duct (31). These findings may also be relevant to trafficking of the V-ATPase in other epithelia such as epididymal clear cells, where the V-ATPase accumulates at the apical membrane in response to PKA (61).

In this study we have identified Ser-175 as the dominant PKA site in the V-ATPase A subunit by two complementary approaches, mass spectrometry and candidate site mutagenesis with subsequent in vitro and in vivo phosphorylation studies performed in HEK-293T cells (Figs. 1-3). Immunolocalization studies performed in HEK-293T cells indicated that in the presence of HCO_3^--containing medium, the WT and S175D mutants accumulated in sub-membrane regions, a finding that mirrored acidification of the culture medium under those transfection conditions (Fig. 4). Furthermore, in the nominal absence of extracellular bicarbonate and Na^+, the proton-secreting activity of HEK-293T cells transfected with the A subunit was largely bafilomycin-sensitive and thus V-ATPase-dependent (Fig. 5). Moreover, under these conditions cells transfected with the WT A subunit responded to PKA activation, whereas PKA phosphorylation-deficient and phospho-mimic Ser-175 mutants were unresponsive to PKA, having either constitutively reduced or elevated V-ATPase activity at the plasma membrane, respectively. PKA-mediated phosphorylation of the A subunit at Ser-175 thus appears to be both necessary and sufficient to confer V-ATPase activity at the plasma membrane in HEK-293 cells. Finally, the immunolocalization studies performed in Clone C cells expressing either WT or S175A mutant A subunit suggest that phosphorylation at Ser-175 is also required for the apical membrane accumulation of the V-ATPase following treatment with PKA activators in a relevant polarized epithelial cell line of intercalated cell characteristics (Fig. 6).

The finding that over-expression of the WT A subunit significantly enhanced V-ATPase-dependent extracellular acidification (Fig. 5) suggests that abundance of the A subunit of the V-ATPase may be rate-limiting for the formation of active V-ATPase holoenzyme complex at the plasma membrane in HEK-293T cells. Of note, the kinetics of assembly of the V-ATPase have largely been investigated in the yeast system (reviewed in

(62)). It has been described that the A subunit of the V_1 sector associates at a faster rate with the V_0 sector *a* subunit than with other subunits of the V_1 sector (reviewed in (1)).

Additional studies are needed to better define the molecular mechanism(s) by which PKA-dependent phosphorylation at Ser-175 in the A subunit is associated with increased plasma membrane accumulation and activity of the V-ATPase. Specifically, it is conceivable that PKA phosphorylation of the A subunit modulates protein-protein interactions within the multi-subunit V-ATPase complex and/or with other interacting proteins involved with cellular trafficking of the pump. For example, the sequence around our identified PKA phosphorylation site is highly conserved in eukaryotes and lies within a so-called 'non-homologous' region (63). This region received its name because it is not present in the F-ATPase β subunit, which otherwise has high homology to the V-ATPase A subunit. It has been described that the highly conserved non-homologous region in the A subunit of the V_1 sector binds to the V_0 sector in a glucose-dependent manner in yeast, where it has been proposed to be a glucose sensor, thereby linking pump function to metabolic status (2,64).

To our knowledge, this study is the first to identify and characterize the functional role of a specific phosphorylation site of any V-ATPase subunit in mammalian cells. Our previous work demonstrated that in addition to PKA, the metabolic-sensing kinase AMPK can directly phosphorylate the A subunit of the V-ATPase (38). An antagonistic regulatory relationship between PKA and AMPK with respect to subcellular localization of the pump in both epididymal clear cells and kidney intercalated cells was also suggested (19). Specifically, AMPK appeared to inhibit PKA-dependent phosphorylation of the A subunit in cells and blocked the PKA-mediated accumulation of the pump at the apical membrane in proton-secreting cells in kidney and epididymis. However, the mechanistic details of how V-ATPase phosphorylation by these two kinases may be translated into an integrated response of the pump to disparate cellular signals is unclear. Specifically, it will be important in future studies to define how PKA-dependent phosphorylation of the pump may couple the sensing of acid-base status to pump activity while AMPK-dependent phosphorylation of the V-ATPase may couple its activity to metabolic and other cellular stresses.

REFERENCES

1. Nelson, N., and Harvey, W. R. (1999) *Physiol Rev* **79**, 361-385
2. Forgac, M. (2007) *Nat Rev Mol Cell Biol* **8**, 917-929
3. Zeidel, M. L., Silva, P., and Seifter, J. L. (1986) *J Clin Invest* **77**, 113-120
4. Gluck, S., and Al-Awqati, Q. (1984) *J Clin Invest* **73**, 1704-1710
5. Gluck, S., and Caldwell, J. (1988) *Am J Physiol* **254**, F71-79
6. Brown, D., Hirsch, S., and Gluck, S. (1988) *J Clin Invest* **82**, 2114-2126
7. Breton, S., Smith, P. J., Lui, B., and Brown, D. (1996) *Nat Med* **2**, 470-472.
8. Marshansky, V., Ausiello, D. A., and Brown, D. (2002) *Curr Opin Nephrol Hypertens* **11**, 527-537
9. Hamm, L. L., and Nakhoul, N. L. (2008) Renal Acidification. in *Brenner and Rector's THE KIDNEY* (Brenner, B. M. ed.), Eight Edition Ed., Saunders Elsevier, Philadelphia. pp 248-279
10. Hamm, L. L., and Hering-Smith, K. S. (1993) *Semin Nephrol* **13**, 246-255
11. Steinmetz, P. R. (1986) *Am J Physiol* **251**, F173-187
12. Karet, F. E., Finberg, K. E., Nelson, R. D., Nayir, A., Mocan, H., Sanjad, S. A., Rodriguez-Soriano, J., Santos, F., Cremers, C. W., Di Pietro, A., Hoffbrand, B. I., Winiarski, J., Bakkaloglu, A., Ozen, S., Dusunsel, R., Goodyer, P., Hulton, S. A., Wu, D. K., Skvorak, A. B., Morton, C. C., Cunningham, M. J., Jha, V., and Lifton, R. P. (1999) *Nat Genet* **21**, 84-90
13. Smith, A. N., Skaug, J., Choate, K. A., Nayir, A., Bakkaloglu, A., Ozen, S., Hulton, S. A., Sanjad, S. A., Al-Sabban, E. A., Lifton, R. P., Scherer, S. W., and Karet, F. E. (2000) *Nat Genet* **26**, 71-75

14. Blomqvist, S. R., Vidarsson, H., Soder, O., and Enerback, S. (2006) *Embo J* **25**, 4131-4141
15. Hays, S., Kokko, J. P., and Jacobson, H. R. (1986) *J Clin Invest* **78**, 1279-1286
16. Gluck, S., and Nelson, R. (1992) *J Exp Biol* **172**, 205-218
17. Pastor-Soler, N., Pietrement, C., and Breton, S. (2005) *Physiology (Bethesda)* **20**, 417-428
18. Wagner, C. A., Finberg, K. E., Breton, S., Marshansky, V., Brown, D., and Geibel, J. P. (2004) *Physiol Rev* **84**, 1263-1314
19. Gong, F., Alzamora, R., Smolak, C., Li, H., Naveed, S., Neumann, D., Hallows, K. R., and Pastor-Soler, N. M. (2010) *Am J Physiol Renal Physiol* **298**, F1162-1169
20. Schwartz, G. J., and Al-Awqati, Q. (1985) *J Clin Invest* **75**, 1638-1644
21. Sautin, Y. Y., Lu, M., Gaugler, A., Zhang, L., and Gluck, S. L. (2005) *Mol Cell Biol* **25**, 575-589
22. Su, Y., Zhou, A., Al-Lamki, R. S., and Karet, F. E. (2003) *J Biol Chem* **278**, 20013-20018
23. Shum, W. W., Da Silva, N., Brown, D., and Breton, S. (2009) *J Exp Biol* **212**, 1753-1761
24. Pech, V., Kim, Y. H., Weinstein, A. M., Everett, L. A., Pham, T. D., and Wall, S. M. (2007) *Am J Physiol Renal Physiol* **292**, F914-920
25. Rothenberger, F., Velic, A., Stehberger, P. A., Kovacikova, J., and Wagner, C. A. (2007) *J Am Soc Nephrol* **18**, 2085-2093
26. Beaulieu, V., Da Silva, N., Pastor-Soler, N., Brown, C. R., Smith, P. J., Brown, D., and Breton, S. (2005) *J Biol Chem* **280**, 8452-8463
27. Breton, S., and Brown, D. (1998) *J Am Soc Nephrol* **9**, 155-166
28. Bastani, B., Purcell, H., Hemken, P., Trigg, D., and Gluck, S. (1991) *J Clin Invest* **88**, 126-136
29. Sabolic, I., Brown, D., Gluck, S. L., and Alper, S. L. (1997) *Kidney Int* **51**, 125-137
30. Schwartz, J. H., Masino, S. A., Nichols, R. D., and Alexander, E. A. (1994) *Am J Physiol* **266**, F94-101
31. Pastor-Soler, N., Beaulieu, V., Litvin, T. N., Da Silva, N., Chen, Y., Brown, D., Buck, J., Levin, L. R., and Breton, S. (2003) *J Biol Chem* **278**, 49523-49529
32. Paunescu, T. G., Da Silva, N., Russo, L. M., McKee, M., Lu, H. A., Breton, S., and Brown, D. (2008) *Am J Physiol Renal Physiol* **294**, F130-138
33. Paunescu, T. G., Ljubojevic, M., Russo, L. M., Winter, C., McLaughlin, M. M., Wagner, C. A., Breton, S., and Brown, D. (2010) *Am J Physiol Renal Physiol* **298**, F643-654
34. Myers, M., and Forgac, M. (1993) *J Biol Chem* **268**, 9184-9186
35. Tuerk, R. D., Thali, R. F., Auchli, Y., Rechsteiner, H., Brunisholz, R. A., Schlattner, U., Wallimann, T., and Neumann, D. (2007) *J Proteome Res* **6**, 3266-3277
36. Dames, P., Zimmermann, B., Schmidt, R., Rein, J., Voss, M., Schewe, B., Walz, B., and Baumann, O. (2006) *Proc Natl Acad Sci U S A* **103**, 3926-3931
37. Voss, M., Vitavska, O., Walz, B., Wieczorek, H., and Baumann, O. (2007) *J Biol Chem* **282**, 33735-33742
38. Hallows, K. R., Alzamora, R., Li, H., Gong, F., Smolak, C., Neumann, D., and Pastor-Soler, N. M. (2009) *Am J Physiol Cell Physiol* **296**, C672-681
39. Pastor-Soler, N. M., Alzamora, R., Naveed, S., Smolak, C., Gong, F., and Hallows, K. R. (2009) *FASEB J* **23**, 602.613
40. Lang, K., Wagner, C., Haddad, G., Burnekova, O., and Geibel, J. (2003) *Cell Physiol Biochem* **13**, 257-262
41. Bhalla, V., Oyster, N. M., Fitch, A. C., Wijngaarden, M. A., Neumann, D., Schlattner, U., Pearce, D., and Hallows, K. R. (2006) *J Biol Chem* **281**, 26159-26169
42. Carattino, M. D., Edinger, R. S., Grieser, H. J., Wise, R., Neumann, D., Schlattner, U., Johnson, J. P., Kleyman, T. R., and Hallows, K. R. (2005) *J Biol Chem* **280**, 17608-17616
43. Djouder, N., Tuerk, R. D., Suter, M., Salvioni, P., Thali, R. F., Scholz, R., Vaahtomeri, K., Auchli, Y., Rechsteiner, H., Brunisholz, R. A., Viollet, B., Makela, T. P., Wallimann, T., Neumann, D., and Krek, W. (2010) *EMBO J* **29**, 469-481
44. Tuerk, R. D., Auchli, Y., Thali, R. F., Scholz, R., Wallimann, T., Brunisholz, R. A., and Neumann, D. (2009) *Anal Biochem* **390**, 141-148

45. Gao, Z., Lei, D., Welch, J., Le, K., Lin, J., Leng, S., and Duhl, D. (2003) *J Pharmacol Exp Ther* **307**, 870-877
46. Hallows, K. R., Fitch AC, Richardson CA, Reynolds PR, Clancy JP, Dagher PC, Witters LA, Kolls JK, Pilewski JM (2006) *J Biol Chem* **281**, 4231-4241
47. Constantinescu, A., Silver, R. B., and Satlin, L. M. (1997) *Am J Physiol* **272**, F167-177
48. Al-Awqati, Q. (1996) *Am J Physiol* **270**, C1571-1580
49. van Adelsberg, J., Edwards, J. C., Takito, J., Kiss, B., and al-Awqati, Q. (1994) *Cell* **76**, 1053-1061
50. Edwards, J. C., van Adelsberg, J., Rater, M., Herzlinger, D., Lebowitz, J., and al-Awqati, Q. (1992) *Am J Physiol* **263**, C521-529
51. van Adelsberg, J., and Al-Awqati, Q. (1986) *J Cell Biol* **102**, 1638-1645
52. Bens, M., Vallet, V., Cluzeaud, F., Pascual-Letallec, L., Kahn, A., Rafestin-Oblin, M. E., Rossier, B. C., and Vandewalle, A. (1999) *J Am Soc Nephrol* **10**, 923-934
53. Bouley, R., Pastor-Soler, N., Cohen, O., McLaughlin, M., Breton, S., and Brown, D. (2005) *Am J Physiol Renal Physiol* **288**, F1103-1112
54. O'Brien, M. C., and Bolton, W. E. (1995) *Cytometry* **19**, 243-255
55. Zippin, J. H., Chen, Y., Nahirney, P., Kamenetsky, M., Wuttke, M. S., Fischman, D. A., Levin, L. R., and Buck, J. (2002) *Faseb J* **15**, 15
56. Ahlin, G., Hilgendorf, C., Karlsson, J., Szigyarto, C. A., Uhlen, M., and Artursson, P. (2009) *Drug Metab Dispos* **37**, 2275-2283
57. Hallows, K. R., Restrepo, D., and Knauf, P. A. (1994) *Am J Physiol* **267**, C1057-1066
58. Boron, W. F. (1986) *Annu Rev Physiol* **48**, 377-388
59. Gluck, S., Cannon, C., and Al-Awqati, Q. (1982) *Proc Natl Acad Sci U S A* **79**, 4327-4331
60. Dobyan, D. C., Magill, L. S., Friedman, P. A., Hebert, S. C., and Bulger, R. E. (1982) *Anat Rec* **204**, 185-197
61. Pastor-Soler, N. M., Hallows, K. R., Smolak, C., Gong, F., Brown, D., and Breton, S. (2008) *Am J Physiol Cell Physiol* **294**, C488-494
62. Kane, P. M. (2006) *Microbiol Mol Biol Rev* **70**, 177-191
63. Shao, E., Nishi, T., Kawasaki-Nishi, S., and Forgac, M. (2003) *J Biol Chem* **278**, 12985-12991
64. Shao, E., and Forgac, M. (2004) *J Biol Chem* **279**, 48663-48670

FOOTNOTES

*We thank Dr. Qais Al-Awqati for the generous gift of Clone C rabbit intercalated cells and Drs. Ossama Kashlan, Ora Weisz, and Thomas Kleyman for helpful discussions. We also thank Alexander and Andrew Zerby for their careful assistance with data management. This study was supported by the National Institutes of Health grants P30 DK079307 "Pittsburgh Kidney Research Center", R01 DK-075048 (to K.R.H.) and R01 DK-084184 (to N.M.P.S.), the American Society of Nephrology Carl W. Gottschalk Research Scholar Award (to N.M.P.S.), the American Heart Association grants AHA 09GRNT2060539 (to N.M.P.S.) and 0825540D (to R.A.), Cystic Fibrosis Foundation Grant CFF R883-CR02 (to C.A.B.), the Swiss National Science Foundation Grant 3100A0-11437/1, the EU FP6 contract LSHM-CT-2004-005272 (EXGENESIS), and a graduate training fellowship ETHIIRA (to R.F.T.).

[1]The abbreviations used are: 6-MB-cAMP, N^6-monobutyryl-cAMP; AMPK, AMP-activated protein kinase; BSA, bovine serum albumin; DMEM, Dulbecco's modified Eagle's medium; HEK, human embryonic kidney; LC–MALDI MS, liquid chromatography matrix-assisted laser desorption/ionization mass spectrometry; FBS, fetal bovine serum; FITC, fluorescein isothiocyanate, IBMX, 3-isobutyl-1-methylxanthine; mPKI, myristoylated protein kinase A inhibitor; NHE, Na^+/H^+ exchanger; PAC, prespotted AnchorChip; pH_o, Extracellular pH, PKA, protein kinase A; ROI, region of interest; S175A, Serine -175 to Alanine; S175D, Serine-175 to Aspartic Acid; sAC, soluble adenylyl cyclase; SEM,

standard error of the mean; TBST, Tris buffered saline-Tween; V-ATPase, Vacuolar H^+-ATPase; WT, wild-type.

FIGURE LEGENDS

Figure 1. Identification of Ser-175 as a major site for PKA phosphorylation in the V-ATPase A subunit. FLAG-A V-ATPase subunit expressed in HEK-293T cells was incubated with a substoichiometric amount of PKA in the presence of [γ-^{32}P]-ATP, the proteins were subjected to SDS-PAGE and the band corresponding to FLAG-A V-ATPase A-subunit was excised. *A*. Autoradiographic film showing the fractionation profile of phosphopeptide mixtures after in-gel-digestion and microfractionation onto PACs. *B*. Analysis by densitometry of individual radioactive spots identified after the microfractionation (shown in *A*) and quantification of the phosphorylated peptides using appropriate standards. The major radioactive peak eluted in fraction E10 and the corresponding phosphorylated peptide was identified by mass spectrometry. *C*. Mouse FLAG-tagged V-ATPase A subunit amino acid sequence highlighting the major peptide phosphorylated by PKA (O21 fraction). *D*. Ser-175 (bold) is part of a highly conserved PKA consensus target phosphorylation site in this peptide.

Figure 2. PKA phosphorylation of the A subunit in vitro occurs at Ser-175. *A*. Typical phospho-screen image (*upper*) revealing the signal of PKA in vitro phosphorylated A subunit compared to the Ser-175 to Ala mutant. The immunoblot blot (*lower*) confirms similar protein expression and loading of the gel for the different conditions. *B*. Quantification of mean (± SEM) V-ATPase A subunit phosphorylation signal normalized for protein loading as assessed by densitometry of Western blot. Compared to wild-type (WT) FLAG-A subunit, the phosphorylation-deficient (Ser to Ala) mutant showed a significant 90-95% decrease in phosphorylation by PKA in vitro (*, $p < 0.05$ relative to WT; $n = 3$**)**.

Figure 3. PKA-dependent *in vivo* phosphorylation of the V-ATPase A subunit in HEK-293T cells occurs at Ser-175. FLAG-tagged WT or S175A mutant A subunit was transfected into HEK-293T cells one day before experimentation, and cells were then incubated with [^{32}P]-orthophosphate for 2 h under control conditions or in the presence of PKA activator (1 mM 6-MB-cAMP; last 20 min of labeling period) or PKA inhibitor (10 µM mPKI; for entire labeling period). Cell lysis, immunoprecipitation using an anti-FLAG antibody, SDS-PAGE, immunoblotting using an anti-FLAG antibody, and exposure of the same membrane to a phospho-screen were then performed as described (38). *A*. Typical phospho-screen image (upper panel) revealing the signal of phosphorylated A subunit in cells expressing FLAG-A-WT subunit (lanes 1-3) or FLAG-A-S175A subunit (lanes 4-6). Lanes 1 and 4 were derived from control-treated cells, lanes 2 and 5 were derived from PKA-stimulated cells, and lanes 3 and 6 were derived from PKA-inhibited cells. The Western blot (lower panel) confirms similar protein expression and loading of the gel for the different conditions. *B*. Quantification of mean (± SEM) V-ATPase A subunit phosphorylation signal relative to FLAG-A-WT control condition and normalized for protein expression. PKA activator increased FLAG-A-WT phosphorylation to ~3.5 times that of the control condition, whereas FLAG-A-S175A mutant subunit phosphorylation was reduced across all conditions to ~0.5 times that of the FLAG-A-WT subunit under the control condition (*, $p < 0.05$ relative to WT control by analysis of variance; n = 3 replicate experiments). *C*. Dot blots using the PKA phosphorylation substrate-specific antibody of whole cell lysate samples taken from cells transfected and treated under the same conditions as shown in *A* and *B* and spotted onto a nitrocellulose filter. *D*. Quantification of mean (± SEM) PKA-phosphorylated substrate signal relative to that FLAG-A-WT-transfected cell lysates under the control condition and normalized to β-actin blot signal re-probed on the same dot blot (not shown). PKA activator 6-MB-cAMP increased PKA-phosphorylated substrate signal to 2-2.5 times that of control (*$p < 0.05$, relative to FLAG-A-WT control; unpaired t-tests), whereas mPKI had no significant effect. As a further control, we measured the levels of [^{32}P]orthophosphate protein labeling in cellular lysates. We did not observe any statistically significant difference across conditions, independently of the A-subunit mutant expressed and of the pharmacologic treatments ($n = 3$ per condition; data not shown).

Figure 4. Expression of WT and mutant V-ATPase A subunit in HEK-293T cells modulates subcellular localization of the A subunit and extracellular pH. HEK-293 cells were transfected with either vector alone (*A*) or FLAG-tagged WT (*B*), S175A (*C*), or S175D (*D*) mutant A subunit one day prior to immunofluorescence staining for expression of FLAG (*green*), concanavalin A coupled to CY3 as a membrane marker (*red*), and TO-PRO-3 nuclear stain (*blue*). Scale bar = 15µm. *E*. Extracellular pH (pH_o) of the culture media from HEK-293T cells transfected with different plasmids after 28-31 h incubation (*, $p < 0.0001$ relative to vector alone; #, $p < 0.0001$ relative to WT; n = 15-18).

Figure 5. Bafilomycin-sensitive, V-ATPase-dependent extracellular acidification is modulated by Ser-175 A subunit mutants and PKA activators in HEK-293T cells. Cells were transfected with vector alone, WT, S175A or S715D mutant FLAG-tagged A subunit for 28-31 h, and the rate of extracellular acidification in each set of transfected cells was measured in a low buffering capacity solution before and after the addition of bafilomycin A1, a specific V-ATPase inhibitor (see Experimental Procedures). The rate of extracellular acidification (-[final buffer pH - initial buffer pH]/Δt) was obtained in the absence or presence of bafilomycin, for cells incubated either with (*A*) or without (*B*) PKA activators (n = 6 for each transfection condition; n = 6 for each treatment condition) (*, $p < 0.005$ relative to vector alone; #, $p < 0.02$ relative to WT).

Figure 6. The phosphorylation-deficient V-ATPase A subunit Ser-175 to Ala mutant does not accumulate at the apical membrane of intercalated cells in response to PKA activators. The Clone C cell line of intercalated cell characteristics was used for independent transient transfections using either WT or S175A A subunit. *A*. Immunoprecipitation using an anti-FLAG antibody (IP-FLAG; *left column*) followed by immunoblotting using antibodies against the *a* (*upper*), A (*middle*), or E (*lower*) V-ATPase subunits revealed that the transfected FLAG-tagged A subunit forms a complex with the native V_0 sector *a* subunit and with the V_1 sector E subunit. No co-immunoprecipitation was observed when no antibody was added to the immunoprcipitation reaction (*center column*). Samples of the whole cell lysate (5%) were also directly immunoblotted for each of the three subunits (*right column*). *B*. One day after transfection with either FLAG-A wild-type subunit (*top panels*) or FLAG-A S175A mutant subunit (*lower panels*), Clone C cells were plated onto Transwell filters. After 4 d the filters were incubated in PBS pH 7.1 with 100 µM 6-MB-cAMP and 0.5 mM IBMX (*right panels*) or with PBS pH 7.1 alone (*left panels*) for 30 min. These incubations were followed by an incubation with concanavalin A coupled to CY3 (*red*) for 5 min in PBS pH 7.1, fixation and immunofluorescence labeling using anti-FLAG antibody (*green*) and TO-PRO-3 nuclear stain (*blue*). Scale bar = 10 µM. *C*. Quantification of V-ATPase-associated MPI ratio of apical ROI-1 (where the A-subunit co-localizes with concanavalin A) and cytoplasmic ROI-2 (A-subunit alone). This ROI-1/ROI-2 ratio under the different conditions reveals a significant PKA-mediated apical V-ATPase accumulation in the cells expressing the WT A subunit compared to cells expressing the S175A mutant (ROI-1/ROI-2 ratio presented as mean (± SEM); *, $p < 0.05$ versus V-ATPase A WT; n = 20-45 cells analyzed for both conditions).

FIGURE 1

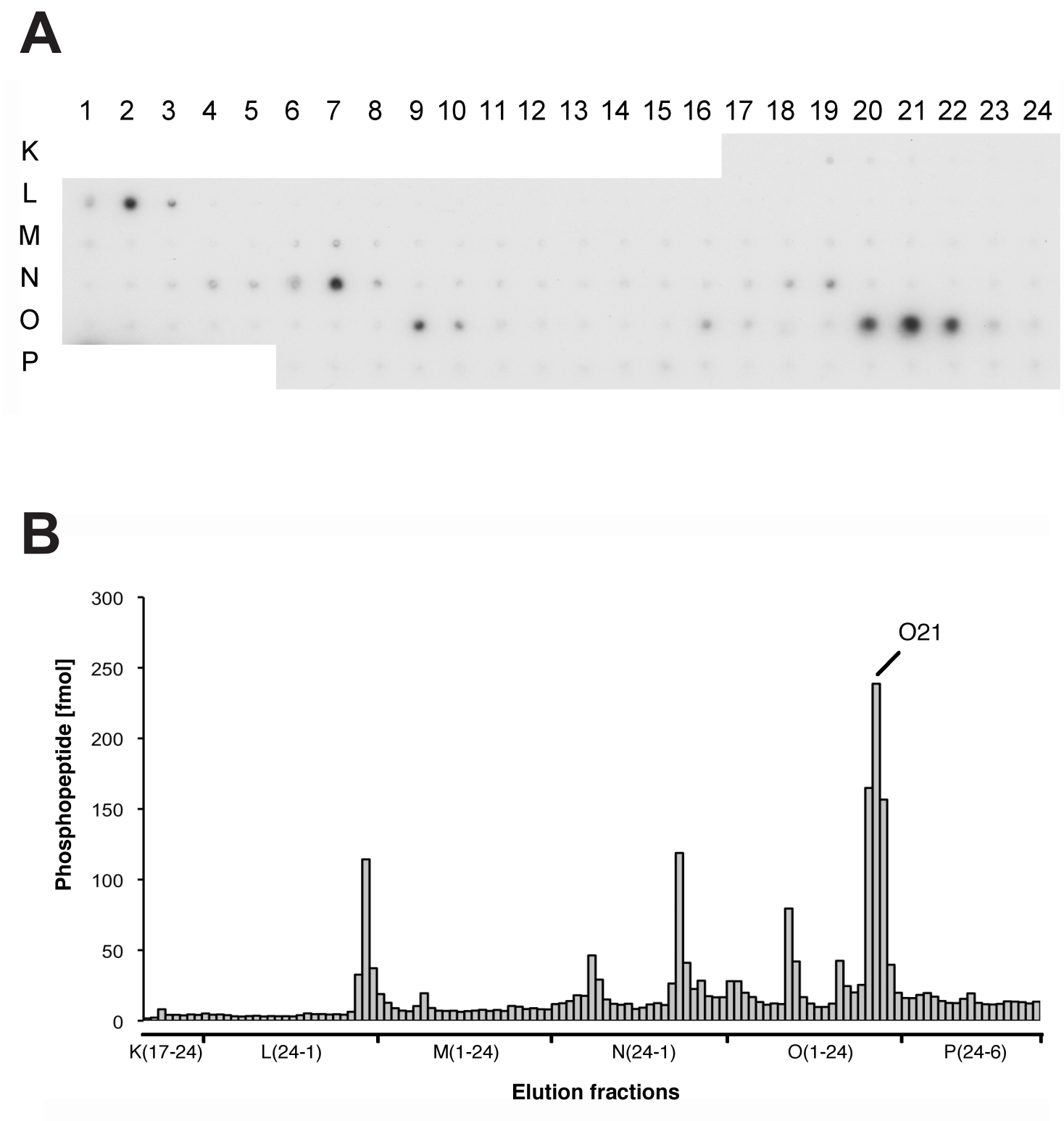

FIGURE 1

C

MDYKDDDDKDFSKLPKIRDEDKESTFGYVHGVSGPVVTACDMAGAAMYELVRVGH
SELVGEIIRLEGDMATIQVYEETSGVSVGDPVLRTGKPLSVELGPGIMGAIFDGI
QRPLSDISSQTQSIYIPRGVNVSALSRDIKWEFIPSKNLRVGSHITGGDIYGIVN
ENSLIKHKIMLPPRNRG**S**VTYIAPPGNYDASDVVLELEFEGVKEKFSMVQVWPVR
QVRPVTEKLPANHPLLTGQRVLDALFPCVQGGTTAIPGAFGCGKTVISQSLSKYS
NSDVIIYVGCGERGNEMSEVLRDFPELTMEVDGKVESIMKRTALVANTSNMPVAA
REASIYTGITLSEYFRDMGYHVSMMADSTSRWAEALREISGRLAEMPADSGYPAY
LGARLASFYERAGRVKCLGNPEREGSVSIVGAVSPPGGDFSDPVTSATLGIVQVF
WGLDKKLAQRKHFPSVNWLISYSKYMRALDEYYDKHFTEFVPLRTKAKEILQEEE
DLAEIVQLVGKASLAETDKITLEVAKLIKDDFLQQNGYTPYDRFCPFYKTVGMLS
NMISFYDMARRAVETTAQSDNKITWSIIREHMGEILYKLSSMKFKDPVKDGEAKI
KADYAQLLEDMQNAFRSLED

D **V-ATPase A subunit Sequence Alignment**

Danio rerio (zebrafish)	160	SLIKHKLMLPPRSRG**T**VTYVAPPGNYDVSDV	190
Xenopus laevis (frog)	160	SLIRHKLMLPPRNRG**T**VTYVAPPGHYDTSDV	190
Rattus norvegicus (rat)	160	SLIKHKIMLPPRSRG**S**VTYIAPPGNYDASDV	190
Mus musculus (mouse)	160	SLIKHKIMLPPRNRG**S**VTYIAPPGNYDASDV	190
Homo sapiens (human)	160	SLIKHKIMLPPRNRG**T**VTYIAPPGNYDTSDV	190

FIGURE 2

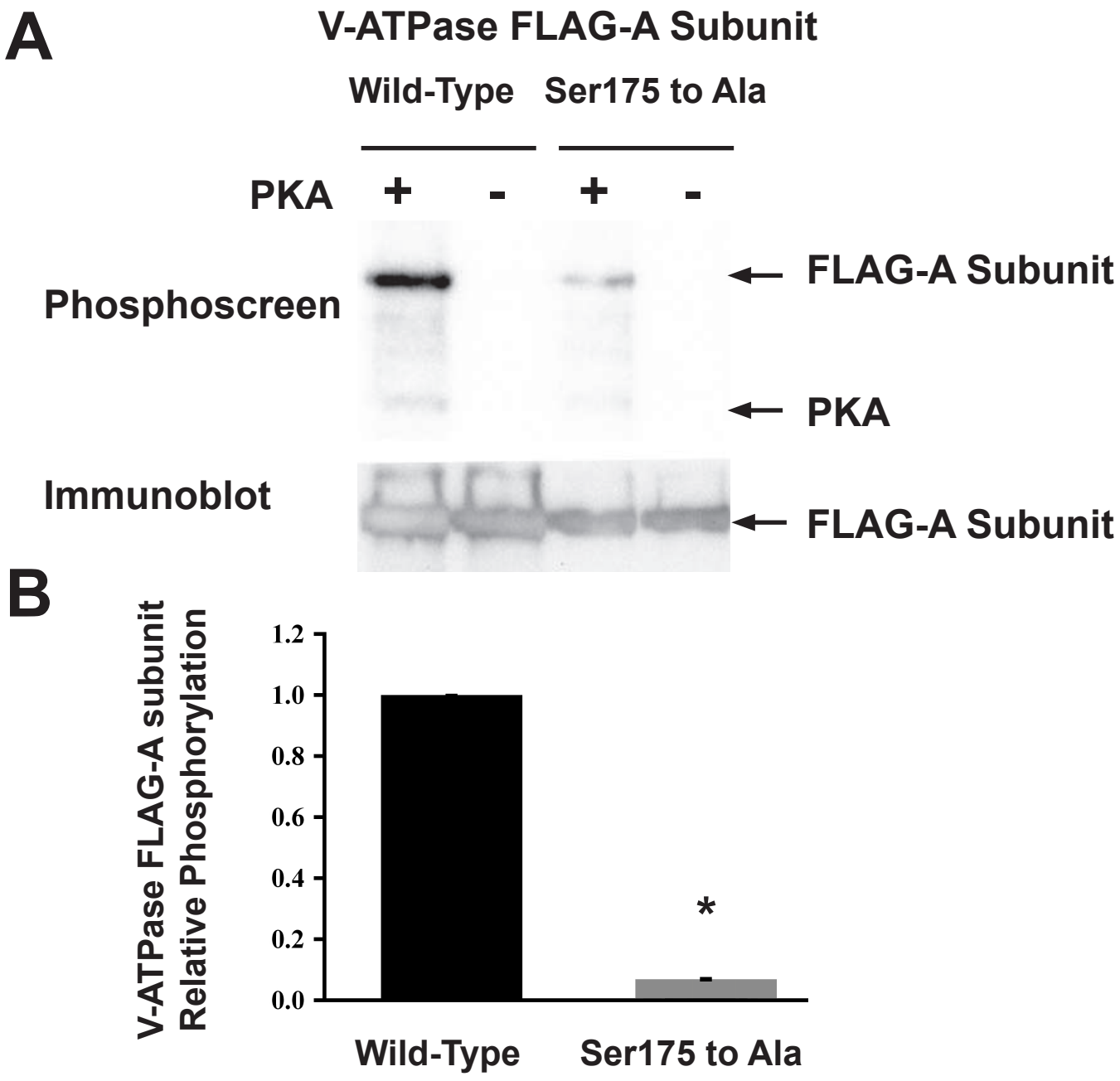

FIGURE 3

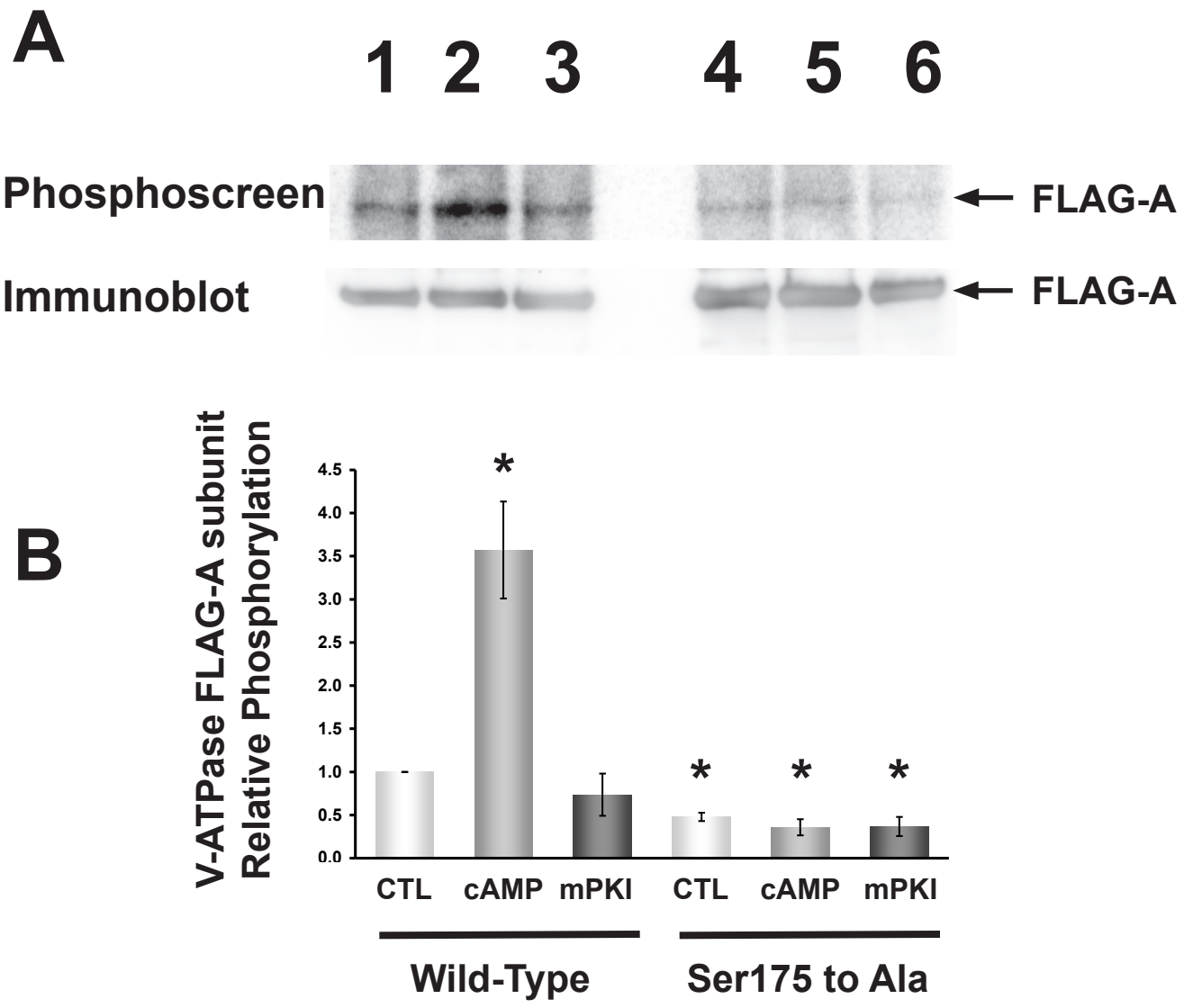

FIGURE 3

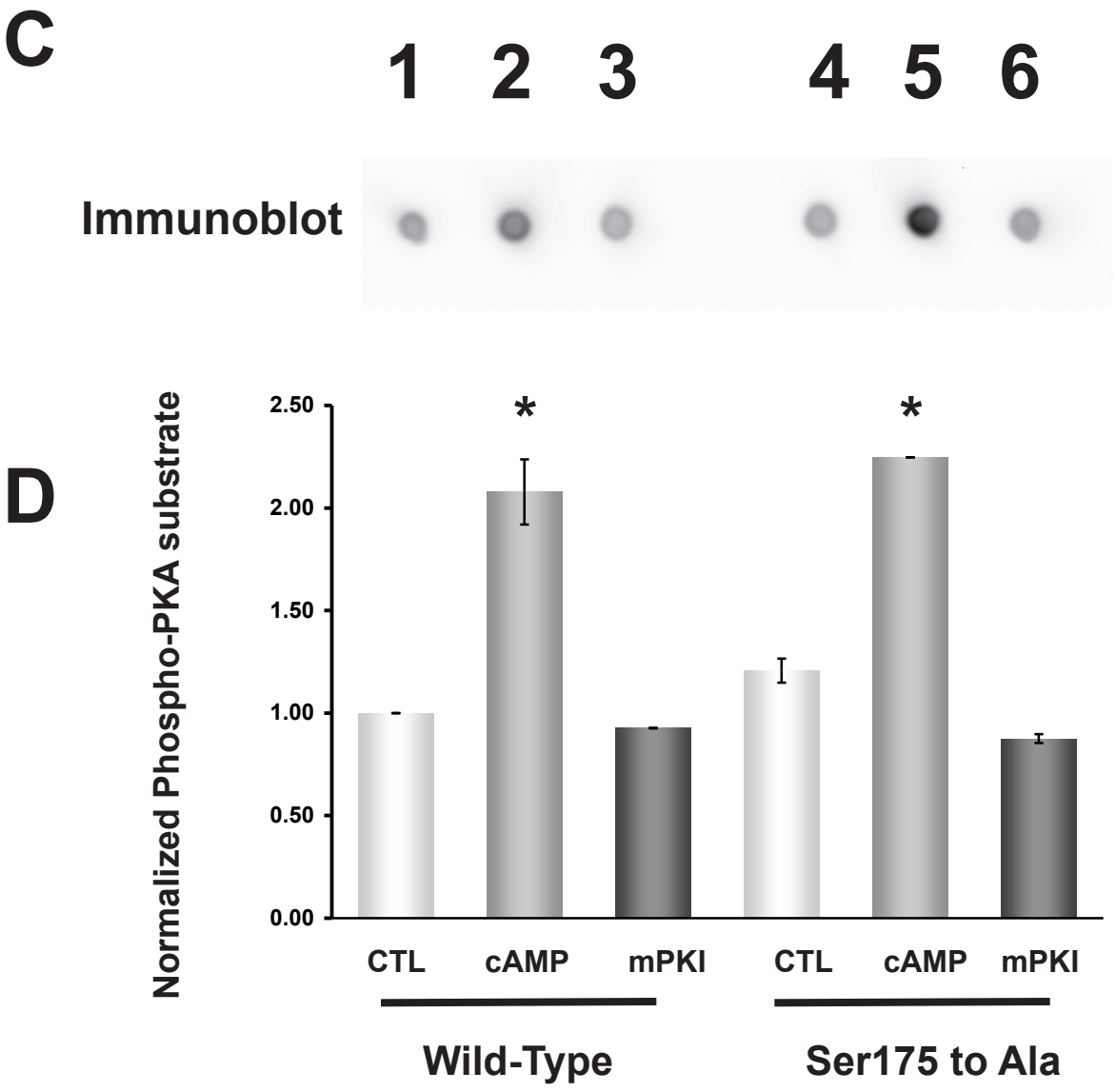

FIGURE 4

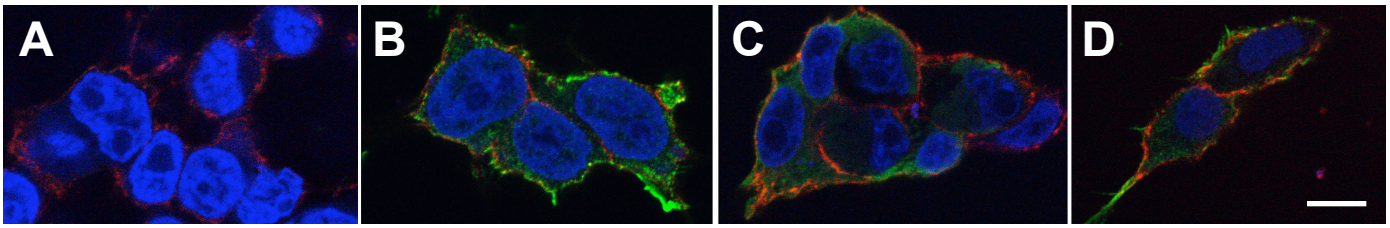

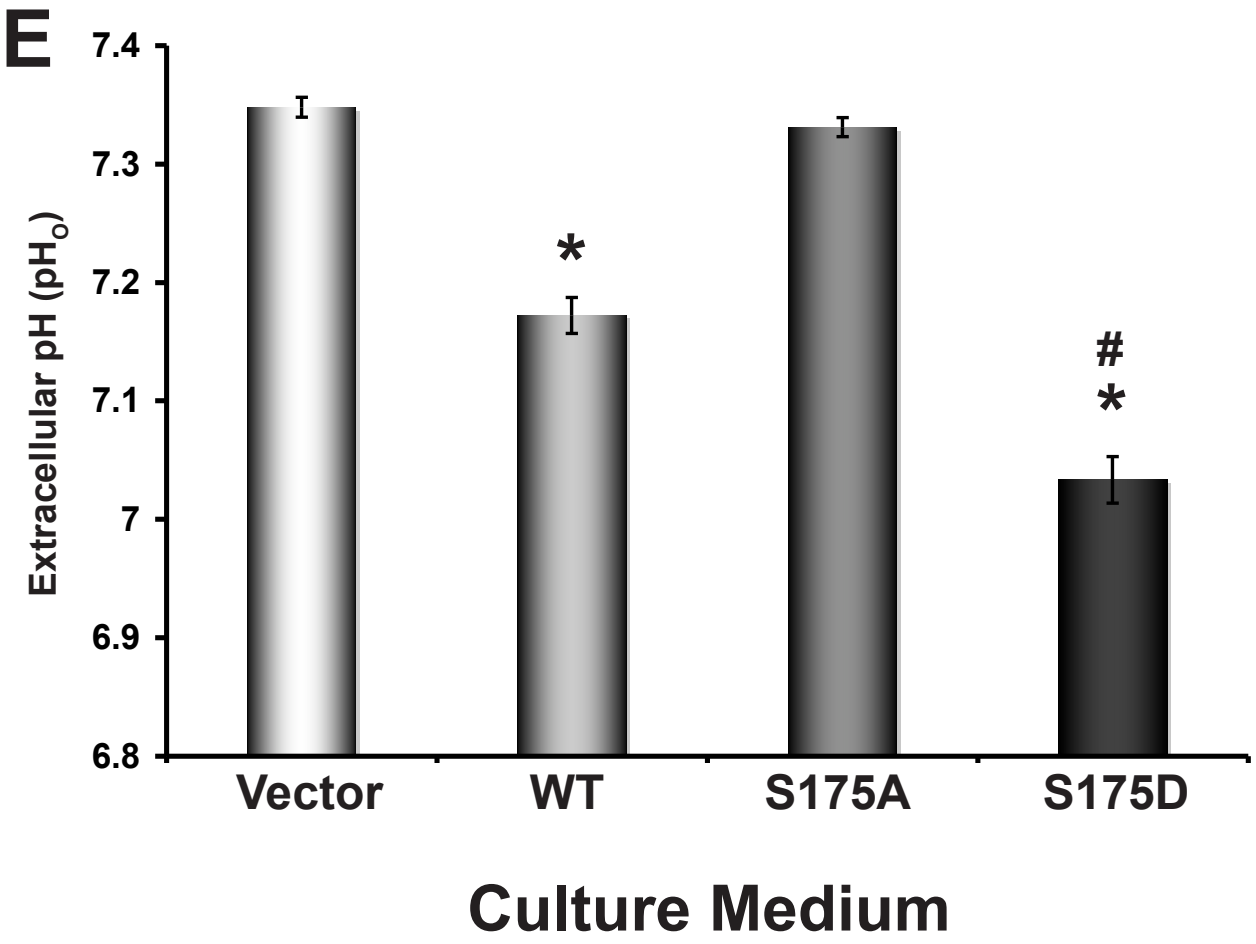

FIGURE 5

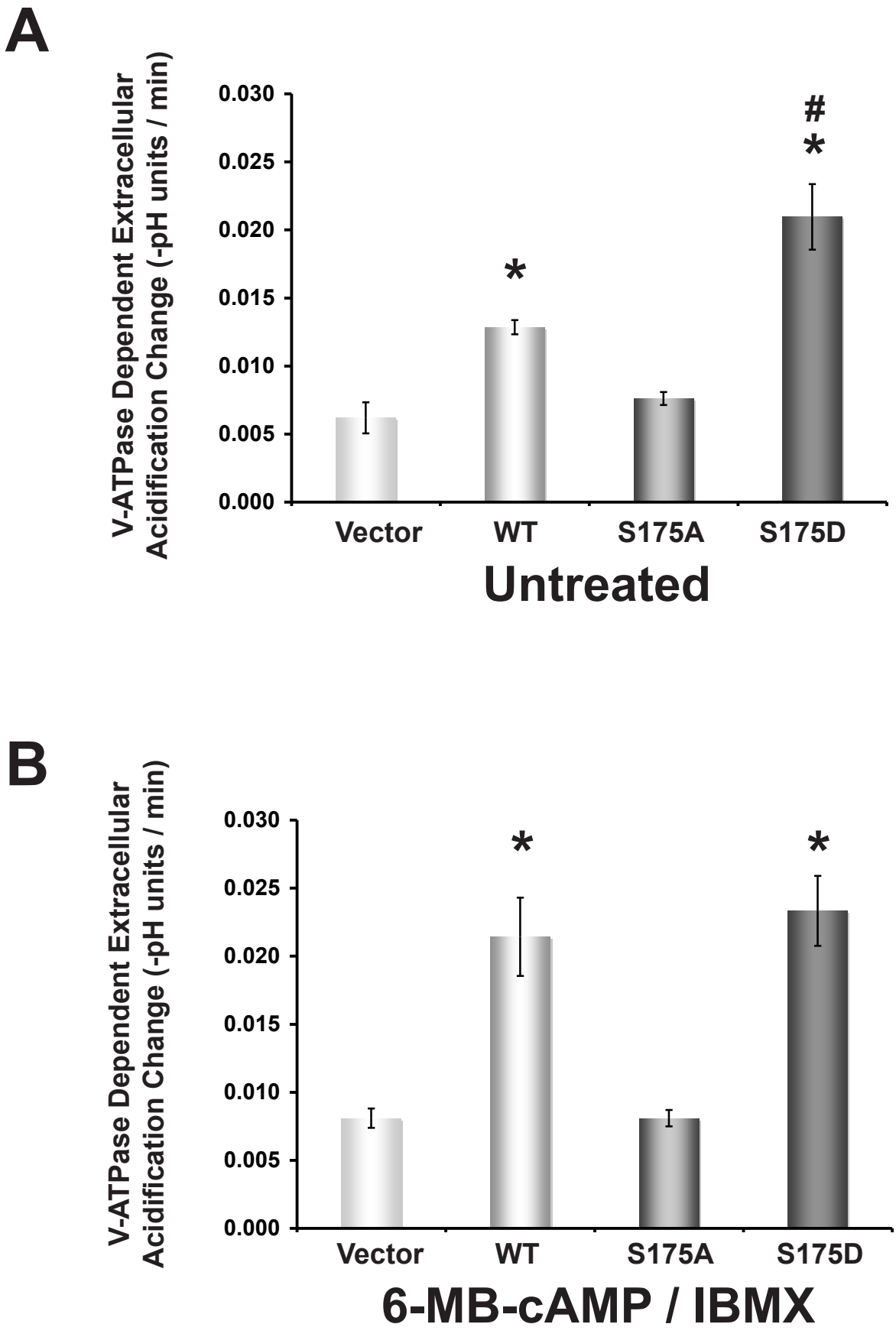

FIGURE 6